A Bioinformatics Study of Structural Perturbation of 3CL-Protease and the HR2-Domain of SARS-CoV-2 Induced by Synergistic Interaction with Ivermectins

Lenin A. González-Paz [1,*] ⓘD , **Carla A. Lossada** [2] ⓘD , **Luis S. Moncayo** [3] ⓘD , **Freddy Romero** [4] ⓘD ,

J. L. Paz [5] ⓘD , **Joan Vera-Villalobos** [6] ⓘD , **Aleivi E. Pérez** [7] ⓘD , **Edgar Portillo** [8] ⓘD , **Ernesto San-Blas** [8] ⓘD ,

Ysaias J. Alvarado [2,*] ⓘD

[1]   Laboratorio de Genética y Biología Molecular (L.G.B.M), Departamento de Biología. Facultad Experimental de Ciencias (F.E.C), Universidad del Zulia (L.U.Z), Maracaibo, Republica Bolivariana de Venezuela
[2]   Laboratorio de Caracterización Molecular y Biomolecular- Centro de Investigación y Tecnología de Materiales (CITeMA)- Instituto Venezolano de Investigaciones Científicas (I.V.I.C)- Zulia, Maracaibo, Republica Bolivariana de Venezuela
[3]   Universidad Católica de Cuenca, Unidad Académica de Salud y Bienestar. Farmacia, Laboratorio de Microbiología. Ecuador
[4]   Department of Medicine, Baylor College of Medicine, Houston, TX, USA
[5]   Departamento de Física, Escuela Politécnica Nacional, Ladrón de Guevara. E11-253,170517; Quito- Ecuador
[6]   Escuela Superior Politécnica del Litoral, Facultad de Ciencias Naturales y Matemáticas, Departamento de Ciencias Químicas y Ambientales, Laboratorio de Síntesis y Caracterización Química, Departamento de Ciencias Biológicas, Facultad de Ciencias de la Salud, Universidad Técnica de Manabí, Ecuador
[7]   Laboratorio de Microbiología General (L.M.G), Departamento de Biología. Facultad Experimental de Ciencias (F.E.C), Universidad del Zulia (L.U.Z), Maracaibo, Republica Bolivariana de Venezuela
[8]   Laboratorio de Protección Vegetal, Centro de Estudios Botánicos y Agroforestales, Instituto Venezolano de Investigaciones Científicas (I.V.I.C)- Zulia, Maracaibo, Republica Bolivariana de Venezuela
*   Correspondence: lgonzalezpaz@gmail.com (L.G.); alvaradoysaias@gmail.com (Y.A.);

Scopus Author ID 6602882448

Abstract: The pandemic caused by SARS-CoV-2 forces drug research to combat it. Ivermectin, an FDA approved antiparasitic drug formulated as a mixture 80:20 of the equipotent homologous 22,23 dihydro ivermectin (B1_a and B1_b), which is known to inhibit SARS-CoV-2 in vitro with a mechanism of action to be defined. It draws attention powerfully that the energetic and structural perturbation that this drug induces by binding on SARS-COV-2 proteins of importance for its proliferation is ill unknown. Hence what we do an exhaustive computational biophysics study to discriminate the best docking of ivermectins to viral proteins and, subsequently, to analyze possible structural alterations with molecular dynamics. The results suggested that ivermectins are capable of docking to the superficial and internal pocket of the 3CL-protease and the HR2-domain, inducing unfolding/folding that change the native conformation in these proteins. In particular, ivermectin binds to the 3CL protease and leads this protein to an unfolded state, whereas the HR2-domain to a more compact conformation in comparison to the native state by refolding when the drug binding to this protein. The results obtained suggest a possible synergistic inhibitory against SARS-COV-2 owing to each role of ivermectins when favorably binding to these viral proteins. Given the importance of the results obtained about this new mechanism of action of ivermectin on SARS-CoV-2, experimental studies are needed that corroborate this proposal.

Keywords: SARS-COV-2; molecular docking; molecular dynamics; COVID-19; ivermectin.

1. Introduction

The first proven clinical case of SARS-CoV-2 was released in December 2019 in Wuhan City, P.R.China [1]. In early May 2020, cases totaled 4,006,257 confirmed cases and 278,892 deaths worldwide [2].The disease caused by this virus has been termed COVID-19. It has been declared by the WHO as a global pandemic [3], and despite the efforts, there is still no vaccine [4]. The study of drugs with known antiviral activity and FDA-approved has been viewed as an attractive and promising way [5,6]. Recently, ivermectin, an drug which really is a mixture in proportion 80:20 of two homologous 22,23 dehydro avermectins B1_a and B1_b (see Figure 1), approved by the FDA for parasitic infections, was reported to have an inhibitory effect on the level of SARS-CoV-2 in vitro, and although ivermectin has been well described to participate in the inhibition of the interaction between the protein integrase (IN) and the heterodimer α/β1 importin (IMP) responsible for the nuclear import of IN in the human immunodeficiency virus -1 (HIV-1) and dengue virus [7,8], and in the inhibition of flavivirus replication by blocking NS3 helicase [9] inactivating enzymes described in SARS [10], and as it is still necessary to define the mechanism that lactone has in vitro inhibitory activity against the new coronavirus as suggested by the authors [11], it would be interesting to assess whether ivermectin has an affinity for other molecular structures than those known and evaluate theoretically if it is capable of inducing structural disturbances once docking, since the inhibitions that have been proposed to explain the mechanism of action are represented by intracellular interactions in other virus, and because there are also open possibilities as a result of possible surface interactions because in this cellular interface there are important protein receptors that can interact with virus proteins before importation as we reported in a preliminary study [12].

On the other hand, theoretical studies have targeted various proteins in SARS-CoV-2, and the docking of several promising compounds has been reported [3,5,13-27]. Involving ivermectin and related virus have been recently reported [9]. However, a theoretical study on structural and energetic changes that ivermectin may induce in SARS-CoV-2 proteins has not been reported.

Are scarce the studies in the literature with target proteins associated with this virus and the MolDock docking algorithm[19], this algorithm is new version docking with more high precision which is based in reparametrization of linear part potential (PLP) [28,29]. To our recognition, we here reported the first study computational biophysics on the energetic and structural changes that induce the two homologous 22,23 dehydro avermectins B1_a and B1_b (ivermectin) to target proteins (3CL-protease, HR2-domain, S2 subunit, spike glycoprotein, RBD spike domain, and NSP15 endoribonuclease) associated with SARS-CoV-2 [30]. Therefore, we conducted a more exhaustive study based on our preliminary results [12] and incorporating more molecular docking algorithms and other scoring functions. MolDock was also used to evaluate the interaction of ivermectins against various functional and surface proteins associated with SARS-CoV-2, as well as more extensive studies of molecular dynamics as a function of time to predict minimum energy structures and a greater number of structural disturbances.

2. Materials and Methods

2.1. Molecular docking screening.

The structures of proteins considered in this work were obtained from Protein Database (https://www.rcsb.org/): 3CL-protease (PDB_ID: 6lu7) [4], HR2-domain (PDB_ID: 6lvn), S2 subunit (PDB_ID: 6lxt), spike glycoprotein (PDB_ID: 6vsb), RBD-domain (PDB_ID: 6vw1), and endoribonuclease NSP15 (PDB_ID: 6vww) [15]. The structures of ivermectin B1_a (ID_6321424) and ivermectin B1_b (ID_6321425) were obtained from PubChem. To simulate ligand-protein binding, complexes were predicted using DockThor (https://dockthor.lncc.br/v2/) using flexibility algorithm, blind docking, and calculating the DockT function. To increase accuracy, 25 runs were made with 10^6 evaluations per run [31]. The thermodynamically most probable and favored position was analyzed with Molegro Molecular Viewer (MMV_7.0.0), calculating the MolDock, Rerank, and PLANTs functions [28] and with AutoDock Vina (ADV) in DINC 2.0 (http://dinc.kavrakilab.org/).

2.2. Molecular dynamics simulation and complementary analysis.

The simulations were carried out with two purposes: 1) to determine the stability of the complex formed by the ligand-protein structure, and 2) obtain conformations for analysis of structural disturbances. A simulated complex was represented by ligand-protein under physiological conditions. For a complex, the system was relaxed through a series of minimization procedures. There were three phases for the simulation: 1) relaxation, 2) equilibrium, and 3) sampling, in which the system progressively heated and equilibrated as recommended [29, 33]. The simulations were run at 100 ns and 4 ns. The myPresto program was used to run all the MD simulations [32]. Molinspiration was used for the bioactivity calculations [34,35] and tools for the SIB [36,37].

3. Results and Discussion

In Table 1 are shown the results obtained of the docking of two homologous 22,23 dehydro avermectins B1_a and B1_b with the protein structures of SARS-CoV-2 considered in this study. These scores represent the classification of binding free energy (ΔG) obtained with DINC 2.0 (ADV Score), DockThor (Dock Score), and MMV (MolDock Scores, Rerank Scores, and PLANTs Scores). Represented by six molecular dockings for ivermectin B1_a and six for B1_b for a total of 12 dockings. The scoring functions predicted a total of six favorable dockings between the proteins and ligands B1_a and B1_b. Curiously, these docking algorithms have not been used for in silico studies associated with SARS-CoV-2. In Table 1 is easy to see that only the Dockt and PLANTs functions predicted favorable docking in all cases (12/12). It can also be observed in this same table 1 that the MolDock and Rerank functions predicted a favorable docking between the ivermectins (B1_a and B1_b) and the 3CL protease (6lu7), HR2-domain (6lvn), and RBD-domain (6vw1) structures. These differences between the algorithms' predictions and the scores of the functions were used to discriminate between the most likely docking.

All the scoring functions agreed that the best thermodynamically favorable coupling was predicted between B1_a and B1_b 3CL-protease and HR2-domain proteins with -11.94 / -7.04 kcal-mol⁻¹ and -9.97 / -26.03 kcal-mol⁻¹ in MolDock, -16.62 / -8.72 kcal-mol⁻¹ and -12.06 / -26.15 kcal-mol⁻¹ in Rerank, -8.64 / -8.29 kcal-mol⁻¹ and -8.29 / -8.24 kcal-mol⁻¹ in DockT, -

39.65 / -31.57 kcal-mol^{-1} and -31.99 / -39.48 kcal-mol^{-1} in PLANTs for ivermectin B1_a / B1_b, respectively. Like the ADV algorithm that predicted docking energy of -1.20 / -2.50 kcal-mol^{-1} and -8.00 / -8.10 kcal-mol^{-1} between lactones B1_a and B1_b and proteins 3CL-protease and HR2-domain, respectively. These dockings were favored by between 80-90% of steric/hydrophobic interactions and were predicted in the same superficial and internal cavities for 3CL-protease and HR2-domain, with each ligand, respectively (see Table 1). It is relevant to make to note that although the docking between ivermectin and 3CL-protease was not predicted in the active catalytic site of the protein, the docking occurred in a superficial pocket adjacent, so it is interesting to study whether it ivermectin can induce in the same way structural disturbances in this important viral protein (see Table 1, Figure 1-2). In this sense, as all the algorithms and scoring functions predicted that the most factible thermodynamically docking occurs between ivermectin and the HR2-domain and 3CL-protease, these structures, as well as the complexes derived from their couplings, were considered for subsequent dynamics analyzes.

It is very important to note that these results obtained are very interesting due to the MolDock algorithm (an extension of the PLP), which contains new hydrogen bonds and electrostatic terms exceed in precision to the other algorithms used in studies related to the protease associated with SARS-CoV-2 [28,29]. Additionally, all the algorithms used considered in this work, except the DockT, predicted that ivermectin B1_a has a higher affinity for the 3CL-protease. In contrast, the homologous B1_b shown a higher affinity for the HR2-domain. These results justify the use of ivermectin as a mixture of homologous molecular B1_a and B1_b [38] because the coupling shows a synergistic action potential. Although it cannot be assured that these results are associated with the antiviral activity described [11, 39]. However, these dockings do not stop attracting attention because the 3CL-protease and the HR2-domain could be considered as the most relevant target protein structures of SARS-CoV-2 in the evaluation of new agents with activity against this disease [5,6,15-21,29,30,40-46]. We, therefore, based on these results, select these two proteins, the 3C-like protease (3CL^{pro}) and the HR2-domain for further investigation. Then, a detailed comparative study was to realize the entre between these proteins and ivermectins B1_a and B1_b (see Table 1, Figure 1-2).

Table 1. Results of the punctuation functions and intermolecular interaction ligand-cavity obtained for docking of each protein selected with ivermectins B1_a and B1_b.

	Ivermectin B1_a_ID_6321424 / Ivermectin B1_b_ID_6321425					
PDB	**DockT Score**	**MolDock Score**	**Rerank Score**	**PLANTs Score**	**ADV Score**	**Interactions**
6vsb	-8.33 / -8.37	5.43 / 5.91	0.79 / 0.31	-23.71 / -24.21	60.40 / 67.10	Asp-950(A)^{HB}, Gly-311(A)^{SI}, Ile-312(A)^{SI}, Ile-664(A)^{SI}, Ser-943(A)^{SI}, Asp-663(A)^{SI}, Lys-310(A)^{SI}, Lys-776(B)^{SI}, Gln-779(B)^{SI}, Glu-661(A)^{SI}, Cys-662(A)^{SI}, Pro-665(A)^{SI}, Val-772(B)^{SI}, Tyr-313(A)^{SI}, Glu-309(A)^{SI}, Asn-953(A)^{SI} / Asp-950(A)^{HB}, Glu-309(A)^{SI}, Asn-953(A)^{SI}, Tyr-313(A)^{SI}, Gly-311(A)^{SI}, Ile-664(A)^{SI}, Val-772(B)^{SI}, Pro-665(A)^{SI}, Cys-662(A)^{SI}, Glu-661(A)^{SI}, Gln-779(B)^{SI}, Ser-943(A)^{SI}, Asp-663(A)^{SI}, Lys-776(B)^{SI}, Lys-310(A)^{SI}
6lxt	-8.13 / -7.26	16.74 / 28.73	5.11 / 20.86	-20.89 / -15.65	-8.10 / -8.50	Asp-1184(F)^{HB}, Ser-939(B)^{SI}, Gln-1180(B)^{SI}, Asp-950(B)^{SI}, Ile-1183(B)^{SI}, Asp-950(B)^{SI}, Gly-946(B)^{SI}, Lys-947(F)^{SI}, Ser-943(F)^{SI}, Ala-942(B)^{SI}, Ser-943(B)^{SI}, Lys-1191(B)^{SI}, Asn-1187(B)^{SI}, Asn-1187(F)^{SI}, Ser-939(F)^{SI}, Glu-1188(F)^{SI}, Lys-1191(F)^{SI} / Asp-95(F)^{HB}, Ser-939(B)^{HB}, Ser-940(B)^{SI}, Lys-1181(A)^{SI}, Asp-950(B)^{SI},

Ivermectin B1_a_ID_6321424 / Ivermectin B1_b_ID_6321425

| PDB	DockT Score	MolDock Score	Rerank Score	PLANTs Score	ADV Score	Interactions
						Lys-947(F)^{SI}, Ser-939(F)^{SI}, Asn-1187(F)^{SI}, Asn-1187(B)^{SI}, Ser-943(B)^{SI}, Asp-1184(F)^{SI}, Gln-1180(F)^{SI}
6lu7	**-8.64 /** **-8.29**	**-11.94 /** **-7.04**	**-16.62 /** **-8.72**	**-39.65 /** **-31.57**	**-1.20 /** **-2.50**	Lys-5^{HB}, Leu-282^{HB}, Glu-288^{SI}, Ser-284^{SI}, Phe-3^{SI}, Phe-291^{SI}, Arg-4^{SI}, Lys-137^{SI}, Val125^{SI}, Gln-127^{SI}, Tyr-126^{SI}, Ser-139^{SI}, Gly-138^{SI}, Ile-281^{SI}, Trp-207^{SI}, Gly-283^{SI} / Lys-5^{HB}, Arg-4^{HB-SI}, Lys-137^{SI}, Tyr-126^{SI}, Gln-127^{SI}, Gly-138^{SI}, Ser-139^{SI}, Phe-3^{SI}, Gly-283^{SI}, Phe-291^{SI}, Leu-282^{SI}, Ser-284^{SI}, Glu-288^{SI}
6lvn	**-8.29 /** **-8.24**	**-9.97 /** **-26.03**	**-12.06 /** **-26.15**	**-31.99 /** **-39.48**	**-8.00 /** **-8.10**	Asp-17(D)$^{HB-SI}$, Gln-13(D)^{HB}, Asn-20(D)^{SI}, Asp-17(C)^{SI}, Asn-20(C)^{SI}, Lys-24(C)^{SI}, Lys-14(D)^{SI}, Arg-18(D)^{SI}, Glu-21(D)^{SI}, Asn-27(B)^{SI}, Ile-16(D)^{SI} / Asp-17(D)^{HB}, Asn-20(D)^{SI}, Va-l10(D)^{SI}, Lys-14(D)^{SI}, Asn-20(C)^{SI}, Glu-21(C)^{SI}, Asp-17(C)^{SI}, Gln-13(D)^{SI}, Glu-2121(D)^{SI}, Lys-24(C)^{SI}
6vw1	-8.32 / -8.25	-10.28 / -7.99	-15.74 / -8.82	-38.23 / -34.57	81.90 / 123.30	Lys-462^{HB-SI}, Tyr-396^{HB-SI}, Glu-516^{HB-SI}, Pro-463^{SI}, Glu-465^{SI}, Arg-355^{SI}, Phe-464^{SI}, Trp-353^{SI}, Arg-466^{SI}, Lys-357^{SI} / Lys-357^{HB-SI}, Lys-462^{SI}, Pro-463^{SI}, Glu-465^{SI}, Phe-464^{SI}, Trp-353^{SI}, Arg-355^{SI}, Glu-516^{SI}, Tyr-396^{SI}, Arg-466^{SI}
6vww	-7.78 / -7.53	17.41 / 13.05	8.10 / 7.55	-24.40 / -23.03	-9.80 / -9.60	Asn-140(B)^{HB}, Asp-79(B)^{HB}, Asp-184(B)^{HB}, Glu-114(A)^{SI}, Pro-119(B)^{SI}, Thr-115(A)^{SI}, Thr-121(B)^{SI}, Va-l183(B)^{SI}, Asp-184(B)^{SI}, Asp-107(A)^{SI}, Ala-95(B)^{SI}, Ile-97(B)^{SI}, His-96(B)^{SI}, Va-l78(B)^{SI}, Leu-120(B)^{SI}, Ile-116(A)^{SI} / Gln-347(B)^{HB}, Asp-79(B)^{SI}, Val-78(B)^{SI}, Gly-77(B)^{SI}, Asn-74(B)^{SI}, Met-272(B)^{SI}, Asn-75(B)^{SI}, Ser-274(B)^{SI}, Thr-326(B)^{SI}, Ile-116(A)^{SI}, Leu-120(B)^{SI}, Pro-119(B)^{SI}

6LU7, 3CL-protease; 6lvn, HR2-domain; 6lxt, S2 subunit; 6vsb, spike glycoprotein; 6vw1, chimeric receptor-binding domain; 6vww, NSP15 ribonuclease; ^{HB}, hydrogen bonds; ^{SI}, steric interactions; ND; not determined; The values to the left and right represent the scores obtained for ivermectins B1_a and B1_b, respectively. Docking with the most probable thermodynamic scores is highlighted in bold. All the binding energies of the scoring functions (DockT, MolDock, Rerank, PLANTs and ADV) are expressed in kcal-mol^{-1}.
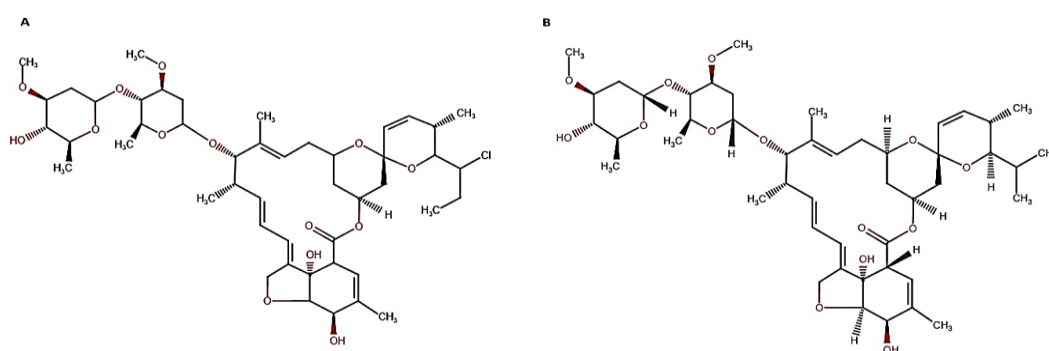
Figure 1. Molecular structure of the two homologous 22,23 dehydro ivermectins considered in this study. A) ivermectin B1_a, and B) ivermectin B1_b.

Additionally, also based on the molecular and structural properties of these drugs, in this work was determined using the Molispiration server that the ligands have an excellent partition coefficient (log$_{Kow}$: 4.08 - 4.58) (Table 2). However, it is essential to note that even though these lactones have a high molecular weight and more than 10 hydrogen bond accepting groups, which may be characteristics incompatible with the Lipinski rules, these molecules comply with the hydrogen bond donor count by having three groups. With a partition

coefficient of less than 5, so they are molecules with difficulties in their permeability, although they can accumulate to the biointerface according to the established standards [47-49]. Furthermore, a low permeability could favor the interaction of the drug with the surface structures of viruses not yet internalized. Also, our study found that these ivermectins do not present the typical characteristics of enzyme or protease inhibitors, as reported in the literature [34] (see Table 2).
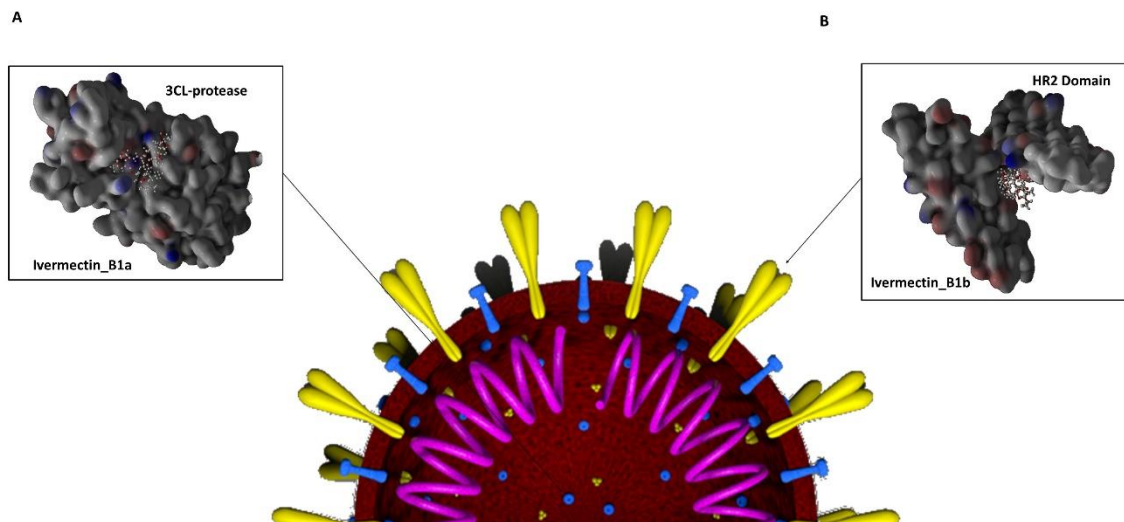
Figure 2. A simplified representation of the functional and structural proteins of SARS-CoV-2 and the complexes protein-ligand obtained theoretically using docking: box A) 3CL protease_B1_a, and box B). HR2-domain_B1_b.

Table 2. Values of the partition coefficient, bioactivity, and the bioaccumulation of the ligands obtained using the Molinspiration server and tools the SIB.

Compounds	MW (g/mol)	log K_{ow}	P-$_{Score}$	E-$_{Score}$	K-$_l$
Ivermectin B1_a	875.10	4.60	-1.90	-2.53	+
Ivermectin B1_b	861.10	4.08	-1.70	-2.40	+

Log_K_{ow}, [49]; P-$_{Score}$, protease inhibitor score [34]; E-$_{Score}$, enzyme inhibitor score [34]; K-$_l$, similarity score with ligands for kinase (Identity= 0.98 [36]).

In this work, we examined the similarity of the two ivermectins B1_a and B1_b studied with the tools the Swiss Institute of Bioinformatics (SIB), and this was found ivermectins do not have the structural and molecular properties of the model drugs for enzyme inhibition of viruses other than SARS-CoV-2 [9]. Its bioactivity could only be traced for P-glycoproteins described previously in the literature[11,37]. But it presents an important structural similarity with ligands for kinase (Identity= 0.98 [36]), an important bioinformatic analysis because signaling pathways involving various kinases are known to be key to the establishment of SARS [50-52], dengue, and MERS [43,53]. In fact, the activity of the ACE2 receptor, which is key to the infectivity of SARS-CoV-2, is affected by the inhibition of certain kinases [43,53,54]. Interesting results because SARS-CoV-2 infects human cells after recognition of the ACE2 receptor [54].

It is also important to consider that chloroquine is an antimalarial drug used for COVID-19 [5,55], also shown favorable thermodynamic docking energies for 3CL-protease [12,15,56,57] and they are capable of inactivating determining kinases, impacting on the reduction of viral titer. It is very interesting to be able to observe if the results theoretical obtained in this study and the similarity between ivermectins (B1_a and B1_b) with ligands with activity to kinases could be compared with the observed with antimalarials and likewise extrapolated to SARS and perhaps other viruses. After predicting fluctuations and positions of the atoms of the ligand-protein docking according to the time, to simulate disturbances of

proteins in the absence and presence of each ligand, we observed that the two homologous B1_a and B1_b present thermodynamically stable interactions. In terms of total energy, the docking of ivermectin_B1_a with 3CL-protease ($\Delta G \leq$ -2900 kcal-mol^{-1}) is more favorable than that observed with ivermectin_B1_b ($\Delta G \leq$ -2800 kcal-mol^{-1}) for 3CL-protease. The B1_a inducing disturbances in thermodynamic stability at 27 ns, unlike the longer time required by B1_b (see Table 3, Figure 3).

Table 3. MD simulations as a function of time of the Ivermectin-protein complexes using the myPresto software package at 100 ns.

Compounds	3CL-protease*		HR2-domain**	
	$E\text{-}Total$ (kcal-mol^{-1})	$Time$ $(ns)/E\text{-}Total$	$E\text{-}Total$ (kcal-mol^{-1})	$Time$ $(ns)/E\text{-}Total$
Ivermectin-B1_a	-2900	27	-2450	96
Ivermectin-B1_b	-2800	86	-2450	34

*, $E\text{-}Total$: -3280 kcal-mol^{-1}, Time/$E\text{-}Total$: 76ns; **, $E\text{-}Total$: -2600 kcal-mol^{-1}, Time/$E\text{-}Total$: 68ns. Reference values calculated in this study.

It is worth mentioning that these values are around to the values reported with other docking scores of candidate agents, including phytochemicals and antimalarial to SARS-CoV-2 [5,12]. Curiously, the results obtained clearly showed that the difference in docking energy in terms of total energy between ivermetics (B1_a and B1_b) and the HR2-domain is negligible. On the other hand, ivermectin B1_b was the one that induced the most notorious alteration in the thermodynamic stability of the HR2-domain. In fact, the time required to reach the most stable structures of lower energy compared to native proteins is shorter within the time scale here considered. In the 100 ns simulation, an abrupt drop to a minimum energy structure of the HR2 structure in the presence of ivermectin B1_b at 34 ns could be observed (see Figure 3F). Both ivermectins (B1_a and B1_b) affected the stability of the two viral proteins, either energy, total energy, or the time required to reach the most stable structures (see Figure 3). In particular, the HR2-domain and 3CL-protease in the native state achieved lower energy structures at 76 ns and 68 ns, in terms of total energy, respectively. The compounds can induce structural and thermodynamic changes in the two enzymes, requiring less time according to the results obtained of molecular dynamics to achieve the stability of the system in the simulated docking (see Table 3, Figure 3).
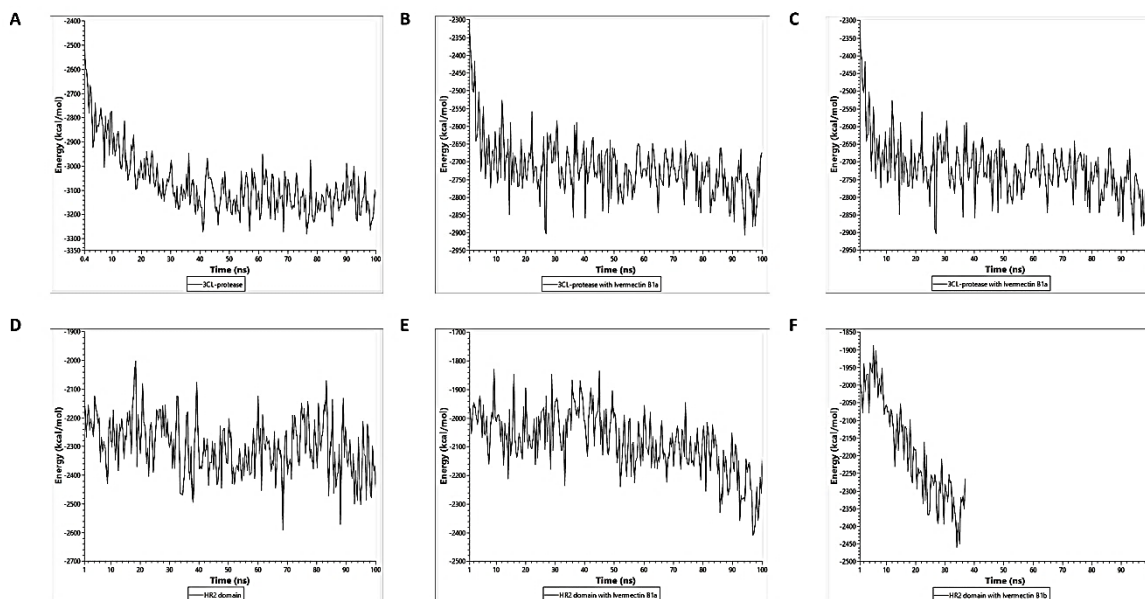
Figure 3. Fluctuation of thermodynamic stability 3CL-protease (A) and HR2-domain (D) in presence of ivermectin B1_a (B and E) and ivermectin B1_b (C and F) at 100 ns, respectively.

Interestingly, we also observed alterations in thermodynamic stability in the early stages of docking, as previously suggested [58] in terms of 4 ns. Mainly, it was observed that the protease in the presence of ivermectin B1_a reached a low energy structure more stable than that induced by B1_b, and in less time than the native one. Similarly, ivermectin B1_b induced a more stable low-energy structure in HR2-domain than that induced by B1_a, although in a longer time than the native one. Results that should not be ignored because they could represent a rapid screening strategy for ligands capable of inducing disturbances in the thermodynamic stability of target proteins in a short time, an aspect that requires further study. In all cases, the low energy structures predicted in the presence of the ligands were thermodynamically less stable than the native conformations. They were reached at different times (see Table 3-4). These results are significant because any of these variations could have an impact on the biological activity of the proteins [59-62].

Table 4. MD simulations as a function of time of the Ivermectin-protein complexes using the myPresto software package at 4 ns.

Compounds	3CL-protease*		HR2-domain**	
	E-Total ($kcal \cdot mol^{-1}$)	Time (ns)/$_{E-Total}$	E-Total ($kcal \cdot mol^{-1}$)	Time (ns)/$_{E-Total}$
Ivermectin B1_a	-2500	2.0	-2055	1.6
Ivermectin B1_b	-2335	1.6	-2080	2.0

*, E_{Total}: -2800 kcal·mol⁻¹, Time/$_{E-Total}$: 2.8ns; **, E_{Total}: -2300 kcal·mol⁻¹, Time/$_{E-Total}$: 1.6ns. Reference values calculated in this study.

Furthermore, the results obtained in terms of thermodynamic stability during bonding correspond to what was observed in the docking, due they show that homologous B1_a has a higher affinity for 3CL. And also that homologous B1_b induced the highest fluctuation in the stability of the HR2-domain under the conditions of this study. A result that also supports the use of these molecules as a mixture for their synergistic action in terms of thermodynamic perturbation of the studied systems (see Table 3-4). In addition, the results revealed that from the early stages of docking the homologous B1_a and B1_b they induce structural perturbation in the viral 3CL-protease and in the HR2-domain. The distances between the residues of Lys-5 and Leu-282, and Gln-13 (chain d) and Gln 13 (chain c) of the 3CL-protease and HR2-domain were used as a reference, respectively, and arbitrarily chosen because they are approximately 3 to 4 Å away from the ligands (see Figure 4).
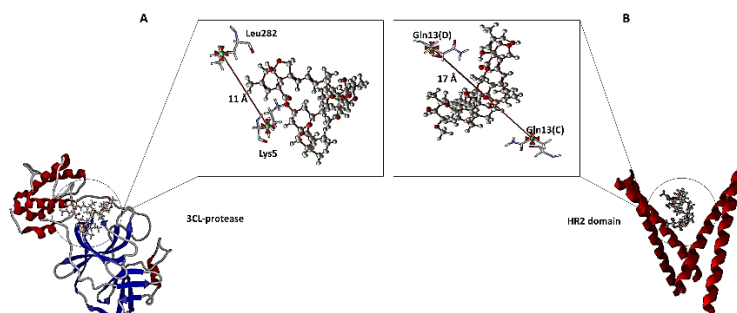
Figure 4. Representation of Docking between residues chosen as a reference for the MD analyzes are shown. A) 3CL-protease-B1_a complex and B) HR2-domain-B1_a complex

Specifically, the ivermectins B1_a and B1_b induce the unfolding of the viral 3CL-protease at very short times of their interaction, but ivermectin B1_a induced the highest structural fluctuation to this viral protease in less than 4 ns according to the simulation, with an unfolding of approximately almost 25% (Figure 5a). Similar results were obtained for ivermectin B1_b but with minor degree unfolding of this protease (Figure 5b). In contrast, the

results showed that the two ivermectins caused the folding of the HR2-domain in the initial stages of docking, with ivermectin B1_b causing the most remarkable structural change in terms of macromolecule folding in a sustained manner with almost 15% folding at the end of the simulation, all compared to the native state and under the time period considered in this study (see Figure 5c and 5d). It is essential to note the relevance of these results because simulations at early timescales that measure the distance between two residues have been shown to can predict changes in protein mobility and structural flexibility, as well as direct interactions of interest to suggest gradual and conformational transitions [58].
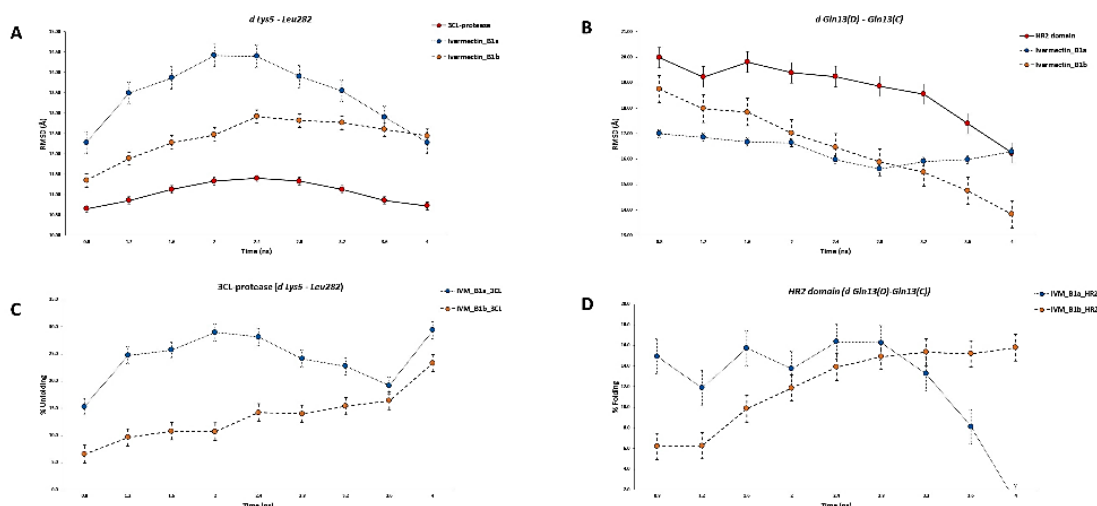
Figure 5. Conformational fluctuation of 3CL-protease and HR2-domain in the presence of ivermectin B1_a (A and C) and ivermectin B1_b (B and D) at 4 ns. Taking the distances between the residues of Lys-5 and Leu-282 as reference for 3CL-protease and Gln-13 (chain d) and Gln-13 (chain c) for HR2-domain. They are arbitrarily chosen because they are at a distance of approximately 4 Å from the ivermectins.

In the same way, we observed that the compounds could induce structural alterations that affect the conformational stability of the two enzymes, in simulations with a larger time scale (Figure 6). We found that like prediction at very early scales of docking, ivermectin B1_a is capable of inducing the most astonishing unfolding of 3CL-protease (Figure 6a).
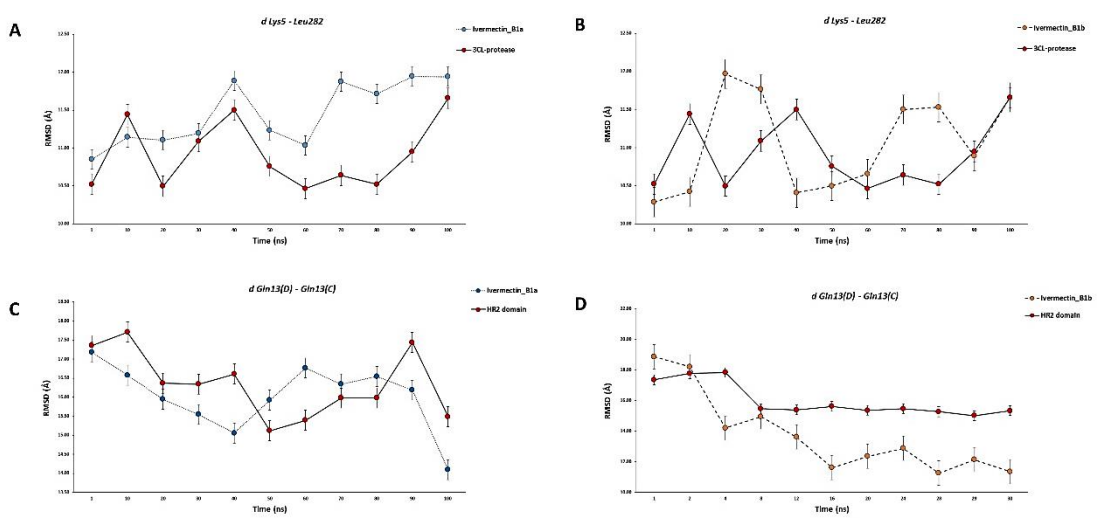
Figure 6. Conformational fluctuation of 3CL-protease and HR2-domain in the presence of ivermectin B1_a (A and C) and ivermectin B1_b (B and D) at 100 ns. Taking the distances between the residues of Lys-5 and Leu-282 as reference for 3CL-protease and Gln-13 (chain d) and Gln-13 (chain c) for HR2-domain. These residues are arbitrarily chosen because they are at a distance of approximately 4 Å from the ivermectins.

In contrast, ivermectin B1_b, on the contrary, induces the greatest folding of the HR2-domain (see Figure 6b). The two ivermectins induced structural changes that coincide with the alterations calculated in terms of thermodynamic stability as a function of time (see Figure 3 and Figure 5-6). In contrast, other works have presented antiviral molecules that, on the one hand, do not significantly influence the structural stability of 3CL-protease, as well as its structural integrity [59,60], and on the other, cause compaction of the protein structure [33,60].

However, It would be very interesting if the future could demonstrate the relationship of these results for the viral protease and the HR2-domain with the biological activity observed for the ivermectin drug. Although, our theoretical results are consistent with thermodynamic alterations and with the best-observed docking. The structural compaction induced by refolding in the HR2-domain as well as the unfolding of the viral protease by ivermectins is interesting, due at the cell membrane as a crowded molecular environment, changes in molecular volume that occur in the biochemical reactions are critical [62], and that the unfolding of proteins has been related to loss of biological activity [63].

Our results are promising because they include FDA-approved drugs that are part of the WHO Essential Drugs [64]. This could be used as a model in more exhaustive bioinformatics studies, such as those reported for other drugs of interest [65,66], including theoretical protocols applied to natural compounds with possible inhibitory effect against SARS-CoV-2 [67,68] or in experimental studies related to the activity of the structure to develop alternatives against this type of virus, especially due to the effect of molecular agglomeration on the conformational dynamics of biomolecules [69], and given that one of the main drawbacks of computational biology is not being able to replicate physiological conditions and therefore more in vivo/in vitro analysis is required to validate and confirm the findings of this study [33,60]. This is important because the SARS-CoV-1 proteins have been reported to show some conformational differences and therefore are not fully compatible docking sites in SARS-CoV-2, which can affect the efficacy of the compounds reused [5,42].

4. Conclusions

The results obtained using theoretical tools showed that ivermectins B1_a and B1_b bind differently of manner to the 3CL-protease and the HR2-domain of SARS-CoV-2 and induce interesting conformational changes in these structures, forcing unfolding/folding of these viral proteins, representing a focus of possible extracellular interactions between this type of compounds with of SARS-CoV-2 proteins before importation. We recommend that experimental studies be carried out on the possible molecular mechanisms described here to establish if there is a relationship with the antiviral activity predicted for this drug against SARS-CoV-2.

Conflicts of Interest

The authors declare no conflict of interest.

References

1. Xu, X.; Chen, P.; Wang, J.; Feng, J.; Zhou, H.; Li, X.; Zhong, W.; Hao, P. Evolution of the novel coronavirus from the ongoing Wuhan outbreak and modeling of its spike protein for risk of human transmission. *Science China Life Sciences* **2020**, *63*, 457-460, https://doi.org/10.1007/s11427-020-1637-5

2. World Health Organization (WHO), Coronavirus disease 2019 (COVID-19): situation report, 112. 2020 https://www.who.int/docs/default-source/coronaviruse/situation-reports/20200511-covid-19-sitrep-112.pdf?sfvrsn=813f2669_2

3. Kadioglu, O.; Saeed, M.; Greten, H.; Efferth, T. Identification of novel compounds against three targets of SARS CoV-2 coronavirus by combined virtual screening and supervised machine learning. *B. World Health Organ* **2020**, https://doi.org/10.2471/BLT.20.255943.

4. Jiang, F.; Deng, L.; Zhang, L.; Cai, Y.; Cheung, C.; Xia, Z. Review of the clinical characteristics of coronavirus disease 2019 (SARS-COV-2). *J. Gen. Intern. Med*. **2020**, *4,* 1-5, https://doi.org/10.1007/s11606-020-05762-w.

5. Chang, Y.; Tung, Y.; Lee, K.; Chen, T.; Hsiao, Y.; Chang, H.; Shih, S. 2020. Potential therapeutic agents for SARS-COV-2 based on the analysis of protease and RNA polymerase docking. *Preprints* **2020**, https://doi.org/10.20944/preprints202002.0242.v1.

6. Contini, A. Virtual screening of an FDA approved drugs database on two SARS-COV-2 coronavirus proteins. *ChemRxiv* **2020**, https://doi.org/10.26434/chemrxiv.11847381.v1.

7. Wagstaff, K.M.; Rawlinson, S.M.; Hearps, A.C.; Jans, D.A. An AlphaScreen®-Based Assay for High-Throughput Screening for Specific Inhibitors of Nuclear Import. *Journal of Biomolecular Screening* **2011**, *16*, 192-200, https://doi.org/10.1177/1087057110390360.

8. Wagstaff, K.; Sivakumaran, H.; Heaton, S.; Harrich, D.; Jans, D. Ivermectin is a specific inhibitor of importin α/β-mediated nuclear import able to inhibit replication of HIV-1 and dengue virus. *Biochem. J.* **2012**, *443,* 851-856, https://doi.org/10.1042/BJ20120150.

9. Mastrangelo, E.; Pezzullo, M.; De Burghgraeve, T.; Kaptein, S.; Pastorino, B.; Dallmeier, K.; de Lamballerie, X.; Neyts, J.; Hanson, A.M.; Frick, D.N.; Bolognesi, M.; Milani, M. Ivermectin is a potent inhibitor of flavivirus replication specifically targeting NS3 helicase activity: new prospects for an old drug. *Journal of Antimicrobial Chemotherapy* **2012**, *67*, 1884-1894, https://doi.org/10.1093/jac/dks147.

10. Tommy, R.T. Drug Targets in Severe Acute Respiratory Syndrome (SARS) Virus and other Coronavirus Infections. *Infectious Disorders - Drug Targets* **2009**, *9*, 223-245, https://doi.org/10.2174/187152609787847659.

11. Caly, L.; Druce, J.D.; Catton, M.G.; Jans, D.A.; Wagstaff, K.M. The FDA-approved drug ivermectin inhibits the replication of SARS-CoV-2 in vitro. *Antiviral Research* **2020**, *178*, https://doi.org/10.1016/j.antiviral.2020.104787.

12. Gonzalez Paz, L.A .; Lossada, C.A .; Moncayo, L.S .; Romero, F .; Paz, J.L .; Vera-Villalobos, J .; Perez, A.E.; San-Blas, E .; Alvarado, Y.J. Molecular Docking and Molecular Dynamic Study of Two Viral Proteins Associated with SARS-CoV-2 with Ivermectin. *Preprints* **2020**, 2020040334, https://doi.org/10.20944 / preprints202004.0334.v1.

13. Liu, X.; Zhang, B.; Jin, Z.; Yang, H.; Rao, Z. The crystal structure of 2019-NCoV main protease in complex with an inhibitor N3. *RCSB Protein Data Bank* **2020**, https://doi.org/10.2210/pdb6LU7/pdb.

14. Khaerunnisa, S.; Kurniawan, H.; Awaluddin, R.; Suhartati, S.; Soetjipto, S. 2020. Potential Inhibitor of SARS-COV-2 Main Protease (Mpro) From Several Medicinal Plant Compounds by Molecular Docking Study. *Preprints* **2020,** https://doi.org/10.20944/preprints202003.0226.v1.

15. Mohammad, F.; Mohsin, A.; Zaw, A.; Tanveer, A.; Waseem, A. Identification of Dietary Molecules as Therapeutic Agents to Combat SARS-COV-2 Using Molecular Docking Studies. *Preprint* (Version 1) available at Research Square, https://doi.org/10.21203/rs.3.rs-19560/v1.

16. Qamar, M.; Alqahtani, S.; Alamri, M.; Chen, L. Structural basis of SARS-CoV-2 3CLpro and anti-SARS-COV-2 drug discovery from medicinal PLANTs. *J. Pharm. Anal.* **2020**, https://doi.org/10.1016/j.jpha.2020.03.009.

17. Sharma, A.; Kaur, I. Eucalyptol (1,8 cineole) from Eucalyptus Essential Oil a Potential Inhibitor of COVID 19 Corona Virus Infection by Molecular Docking Studies. *Preprints* **2020,** https://doi.org/10.20944/preprints202003.0455.v1.

18. Chandel, V.; Raj, S.; Rathi, B.; Kumar, D. In Silico Identification of Potent SARS-COV-2 Main Protease Inhibitors from FDA Approved Antiviral Compounds and Active Phytochemicals through Molecular Docking: A Drug Repurposing Approach. *Preprints* **2020,** https://doi.org/10.20944/preprints202003.0349.v1.

19. Adem, S.; Eyupoglu, V.; Sarfraz, I.; Rasul, A.; Ali, M. Identification of Potent SARS-COV-2 Main Protease (Mpro) Inhibitors from Natural Polyphenols: An in Silico Strategy Unveils a Hope against CORONA. *Preprints* **2020**, https://doi.org/10.20944/preprints202003.0333.v1.

20. Gentile, D.; Patamia, V.; Scala, A.; Sciortino, M.T.; Piperno, A.; Rescifina, A. Inhibitors of SARS-CoV-2 Main Protease from a Library of Marine Natural Products: A Virtual Screening and Molecular Modeling Study. *Preprints* **2020,** https://doi.org/10.20944/preprints202003.0372.v1.

21. Sun, N.; Wong, W.; Guo, J. Prediction of Potential 3CLpro-Targeting Anti-SARS-CoV-2 Compounds from Chinese Medicine. *Preprints* 2020, https://doi.org/10.20944/preprints202003.0247.v1.

22. Muralidharan, N.; Sakthivel, R.; Velmurugan, D.; Gromiha, M.M. Computational studies of drug repurposing and synergism of lopinavir, oseltamivir and ritonavir binding with SARS-CoV-2 protease against COVID-19. *Journal of Biomolecular Structure and Dynamics* 2020, 1-6, https://doi.org/10.1080/07391102.2020.1752802.

23. Sinha, S.K.; Shakya, A.; Prasad, S.K.; Singh, S.; Gurav, N.S.; Prasad, R.S.; Gurav, S.S. An in-silico evaluation of different Saikosaponins for their potency against SARS-CoV-2 using NSP15 and fusion spike glycoprotein as targets. *Journal of Biomolecular Structure and Dynamics* 2020, 1-12, https://doi.org/10.1080/07391102.2020.1762741.

24. Joshi, R.S.; Jagdale, S.S.; Bansode, S.B.; Shankar, S.S.; Tellis, M.B.; Pandya, V.K.; Chugh, A.; Giri, A.P.; Kulkarni, M.J. Discovery of potential multi-target-directed ligands by targeting host-specific SARS-CoV-2 structurally conserved main protease. *Journal of Biomolecular Structure and Dynamics* 2020, 1-16, https://doi.org/10.1080/07391102.2020.1760137.

25. Enmozhi, S.K.; Raja, K.; Sebastine, I.; Joseph, J. Andrographolide as a potential inhibitor of SARS-CoV-2 main protease: an in silico approach. *Journal of Biomolecular Structure and Dynamics* 2020, 1-10, https://doi.org/10.1080/07391102.2020.1760136.

26. Elfiky, A.A. SARS-CoV-2 RNA dependent RNA polymerase (RdRp) targeting: an in silico perspective. *Journal of Biomolecular Structure and Dynamics* 2020, 1-9, https://doi.org/10.1080/07391102.2020.1761882.

27. Wahedi, H.M.; Ahmad, S.; Abbasi, S.W. Stilbene-based natural compounds as promising drug candidates against COVID-19. *Journal of Biomolecular Structure and Dynamics* 2020, 1-16, https://doi.org/10.1080/07391102.2020.1762743.

28. homsen, R.; Christensen, M.H. MolDock: A New Technique for High-Accuracy Molecular Docking. *Journal of Medicinal Chemistry* 2006, *49*, 3315-3321, https://doi.org/10.1021/jm051197e.

29. Wang, J. Fast Identification of possible drug treatment of coronavirus disease-19 (SARS-COV-2) through computational drug repurposing study. *ChemRxiv* 2020, https://doi.org/10.26434/chemrxiv.11875446.v1.

30. Alamri, M.A.; Tahir ul Qamar, M.; Alqahtani, S.M. Pharmacoinformatics and Molecular Dynamic Simulation Studies Reveal Potential Inhibitors of SARS-CoV-2 Main Protease 3CLpro. *Preprints* 2020, https://doi.org/10.20944/preprints202002.0308.v1.

31. Santos, K.B.; Guedes, I.A.; Karl, A.L.M.; Dardenne, L.E. Highly Flexible Ligand Docking: Benchmarking of the DockThor Program on the LEADS-PEP Protein–Peptide Data Set. *Journal of Chemical Information and Modeling* 2020, *60*, 667-683, https://doi.org/10.1021/acs.jcim.9b00905.

32. Kasahara, K.; Ma, B.; Goto, K.; Dasgupta, B.; Higo, J.; Fukuda, I.; Mashimo, T.; Akiyama, Y.; Nakamura, H. myPresto/omegagene: a GPU-accelerated molecular dynamics simulator tailored for enhanced conformational sampling methods with a non-Ewald electrostatic scheme. *Biophysics and Physicobiology* 2016, *13*, 209-216, https://doi.org/10.2142/biophysico.13.0_209.

33. Khan, S.A.; Zia, K.; Ashraf, S.; Uddin, R.; Ul-Haq, Z. Identification of chymotrypsin-like protease inhibitors of SARS-CoV-2 via integrated computational approach. *Journal of Biomolecular Structure and Dynamics* 2020, 1-13, https://doi.org/10.1080/07391102.2020.1751298.

34. Cheminformatics, M. Molinspiration. Web-enabled software for large-scale calculation of molecular properties and database searches. *Free online molecular descriptor calculations* 2020.

35. Reena Roy, D.; Kandagalla, S.; Krishnappa, M. Exploring the ethnomycological potential of Lentinus squarrosulus Mont. through GC–MS and chemoinformatics tools. *Mycology* 2020, *11*, 78, https://doi.org/10.1080/21501203.2019.1707724.

36. Zoete, V.; Daina, A.; Bovigny, C.; Michielin, O. SwissSimilarity: A Web Tool for Low to Ultra High Throughput Ligand-Based Virtual Screening. *Journal of Chemical Information and Modeling* 2016, *56*, 1399-1404, https://doi.org/10.1021/acs.jcim.6b00174.

37. Daina, A.; Michielin, O.; Zoete, V. SwissADME: a free web tool to evaluate pharmacokinetics, drug-likeness and medicinal chemistry friendliness of small molecules. *Scientific Reports* 2017, *7*, https://doi.org/10.1038/srep42717.

38. Yazwinski, T.A.; Williams, M.; Greenway, T.; Tilley, W. Anthelmintic activities of ivermectin against gastrointestinal nematodes of cattle. *Am J Vet Res* 1981, *42*, 481-482.

39. Varghese, F.S.; Kaukinen, P.; Gläsker, S.; Bespalov, M.; Hanski, L.; Wennerberg, K.; Kümmerer, B.M.; Ahola, T. Discovery of berberine, abamectin and ivermectin as antivirals against chikungunya and other alphaviruses. *Antiviral Research* 2016, *126*, 117-124, https://doi.org/10.1016/j.antiviral.2015.12.012.

40. Elshabrawy, H.A.; Coughlin, M.M.; Baker, S.C.; Prabhakar, B.S. Human Monoclonal Antibodies against Highly Conserved HR1 and HR2-domains of the SARS-CoV Spike Protein Are More Broadly Neutralizing. *PLOS ONE* 2012, *7*, https://doi.org/10.1371/journal.pone.0050366.

41. Arya, R.; Das, A.; Prashar, V.; Kumar, M. Potential inhibitors against papain-like protease of novel coronavirus (SARS-CoV-2) from FDA approved drugs. *ChemRxiv* 2020, https://doi.org/10.26434/chemrxiv.11860011.v2.

42. Bzowka, M.; Mitusinska, K.; Raczynska, A.; Samol, A.; Tuszynski, J.; Gora, A. Molecular Dynamics Simulations Indicate the SARS-COV-2 Mpro Is Not a Viable Target for Small-Molecule Inhibitors Design. *bioRxiv* **2020.**

43. Choudhary, S.; Malik, Y.; Tomar, S.; Tomar, S. Identification of SARS-CoV-2 Cell Entry Inhibitors by Drug Repurposing Using in Silico Structure-Based Virtual Screening Approach. *ChemRxiv* **2020,** https://doi.org/10.26434/chemrxiv.12005988.v2.

44. Sekhar, T. Virtual Screening based prediction of potential drugs for SARS-COV-2. *Preprints* **2020**, https://doi.org/10.20944/preprints202002.0418.v2.

45. Xia, S.; Liu, M.; Wang, C.; Xu, W.; Lan, Q.; Feng, S.; Qi, F.; Bao, L.; Du, L.; Liu, S.; Qin, C.; Sun, F.; Shi, Z.; Zhu, Y.; Jiang, S.; Lu, L. Inhibition of SARS-CoV-2 (previously 2019-nCoV) infection by a highly potent pan-coronavirus fusion inhibitor targeting its spike protein that harbors a high capacity to mediate membrane fusion. *Cell Res.* **2020**, 1-13, https://doi.org/10.1038/s41422-020-0305-x.

46. Zhang, J.; Shen, X.; Yan, Y.; Yan, W.; Cheng, Y. Discovery of anti-SARS-CoV-2 agents from commercially available flavor via docking screening. *OSF Preprints* **2020**, https://doi.org/10.31219/osf.io/vjch2.

47. Leo, A.; Hansch, C.; Elkins, D. Partition coefficients and their uses. *Chemical Reviews* **1971**, *71*, 525-616, https://doi.org/10.1021/cr60274a001.

48. Ghose, A.K.; Viswanadhan, V.N.; Wendoloski, J.J. A Knowledge-Based Approach in Designing Combinatorial or Medicinal Chemistry Libraries for Drug Discovery. 1. A Qualitative and Quantitative Characterization of Known Drug Databases. *Journal of Combinatorial Chemistry* **1999**, *1*, 55-68, https://doi.org/10.1021/cc9800071.

49. Bhal, S. LogP—Making sense of the value. *Advanced chemistry development, Toronto, ON, Canada* **2007,** 1-4.

50. Mizutani, T.; Fukushi, S.; Saijo, M.; Kurane, I.; Morikawa, S. Importance of Akt signaling pathway for apoptosis in SARS-CoV-infected Vero E6 cells. *Virology* **2004**, *327*, 169-174, https://doi.org/10.1016/j.virol.2004.07.005.

51. Mizutani, T.; Fukushi, S.; Saijo, M.; Kurane, I.; Morikawa, S. JNK and PI3k/Akt signaling pathways are required for establishing persistent SARS-CoV infection in Vero E6 cells. *Biochimica et Biophysica Acta (BBA) - Molecular Basis of Disease* **2005**, *1741*, 4-10, https://doi.org/10.1016/j.bbadis.2005.04.004.

52. Krähling, V.; Stein, D.A.; Spiegel, M.; Weber, F.; Mühlberger, E. Severe Acute Respiratory Syndrome Coronavirus Triggers Apoptosis via Protein Kinase R but Is Resistant to Its Antiviral Activity. *J Virol* **2009**, *83*, 2298-2309, https://doi.org/10.1128/JVI.01245-08.

53. Coleman, C.; Sisk, J.; Mingo, R.; Nelson, E.; White, J.; Frieman, M. Abelson Kinase Inhibitors Are Potent Inhibitors of Severe Acute Respiratory Syndrome Coronavirus and Middle East Respiratory Syndrome Coronavirus Fusion. *J Virol* **2016**, *90*, 8924-8933, https://doi.org/10.1128/JVI.01429-16.

54. Velavan, T.P.; Meyer, C.G. The COVID-19 epidemic. *Tropical Medicine & International Health* **2020**, *25*, 278-280, https://doi.org/10.1111/tmi.13383.

55. Devaux, C.A.; Rolain, J.-M.; Colson, P.; Raoult, D. New insights on the antiviral effects of chloroquine against coronavirus: what to expect for COVID-19? *International Journal of Antimicrobial Agents* **2020**, *55*, https://doi.org/10.1016/j.ijantimicag.2020.105938.

56. Gautret, P.; Lagier, J.; Parola, P.; Meddeb, L.; Mailhe, M.; Doudier, B.; Honoré, S. Hydroxychloroquine and azithromycin as a treatment of SARS-COV-2: results of an open-label non-randomized clinical trial. *Int. J. Antimicrob. Agents* **2020**, https://doi.org/10.1016/j.ijantimicag.2020.105949.

57. Wang, M.; Cao, R.; Zhang, L.; Yang, X.; Liu, J.; Xu, M.; Shi, Z.; Hu, Z.; Zhong, W.; Xiao, G. Remdesivir and chloroquine effectively inhibit the recently emerged novel coronavirus (2019-nCoV) in vitro. *Cell Research* **2020**, *30*, 269-271, https://doi.org/10.1038/s41422-020-0282-0.

58. Aci-Sèche, S.; Ziada, S.; Braka, A.; Arora, R.; Bonnet, P. Advanced molecular dynamics simulation methods for kinase drug discovery. *Future Medicinal Chemistry* **2016**, *8*, 545-566, https://doi.org/10.4155/fmc.16.9.

59. Muralidharan, N.; Sakthivel, R.; Velmurugan, D.; Gromiha, M.M. Computational studies of drug repurposing and synergism of lopinavir, oseltamivir and ritonavir binding with SARS-CoV-2 protease against COVID-19. *Journal of Biomolecular Structure and Dynamics* **2020**, 1-6, https://doi.org/10.1080/07391102.2020.1752802.

60. Khan, R.J.; Jha, R.K.; Amera, G.M.; Jain, M.; Singh, E.; Pathak, A.; Singh, R.P.; Muthukumaran, J.; Singh, A.K. Targeting SARS-CoV-2: a systematic drug repurposing approach to identify promising inhibitors against 3C-like proteinase and 2′-O-ribose methyltransferase. *Journal of Biomolecular Structure and Dynamics* **2020**, 1-40, https://doi.org/10.1080/07391102.2020.1753577.

61. Tzeng, S.R.; Kalodimos, C.G. Protein activity regulation by conformational entropy. *Nature* **2012**, *488*, 236-240, https://doi.org/10.1038/nature11271.

62. Gomez, D.; Huber, K.; Klumpp, S. On Protein Folding in Crowded Conditions. *The Journal of Physical Chemistry Letters* **2019**, *10*, 7650-7656, https://doi.org/10.1021/acs.jpclett.9b02642.

63. Askin, S.; Bond, T.E.H.; Sorenson, A.E.; Moreau, M.J.J.; Antony, H.; Davis, R.A.; Schaeffer, P.M. Selective protein unfolding: a universal mechanism of action for the development of irreversible inhibitors. *Chemical Communications* **2018**, *54*, 1738-1741, https://doi.org/10.1039/C8CC00090E.

64. World Health Organization (WHO). World Health Organization model list of essential medicines: 21st list 2019. Geneva: World Health Organization. hdl:10665/325771. WHO/MVP/EMP/IAU/2019.06. License: CC BY-NC-SA 3.0 IGO, 2019, https://apps.who.int/iris/bitstream/handle/10665/325771/WHO-MVP-EMP-IAU-2019.06-eng.pdf..

65. Fatonah, A.; Tambunan, U.; Pamungkas, W.; Dewanto, G.; Wicaksono, I. Discovery of GPX4 inhibitor by molecular docking simulation as a potential ferroptosis inducer. *Biointerface Res. Appl. Chem.* **2020**, *10,* 4929-4933, https://doi.org/10.33263/BRIAC101.929933.

66. Choudhary, S.; Malik, Y.; Tomar, S.; Tomar, S. Identification of SARS-CoV-2 cell entry inhibitors by drug repurposing using in silico structure-based virtual screening approach. *Chemrxiv* **2020**, https://doi.org/10.26434/chemrxiv.12005988.v2.

67. Sampangi-Ramaiah, M.; Vishwakarma, R.; Shaanker, R. Molecular docking analysis of selected natural products from PLANTs for inhibition of SARS-CoV-2 main protease. *Curr. Sci.* **2020**, *118*, 1087-1092, https://doi.org/10.18520/cs/v118/i7/1087-1092.

68. Aanouz, I.; Belhassan, A.; El Khatabi, K.; Lakhlifi, T.; El Idrissi, M.; Bouachrine, M. Moroccan Medicinal PLANTs as inhibitors of COVID-19: Computational investigations. *J. Biomol. Struct. Dyn.* **2020,** (just-accepted), 1-12, https://doi.org/10.1080/07391102.2020.1758790.

69. Kakati, M.; Das, D., Das, P.; Sanjeev, A.; Mattaparthi, V. Effect of ethanol as molecular crowding agent on the conformational dynamics of α-synuclein. *Lett. Appl. NanoBioScience*, **2020**, 9, 779 – 783, https://doi.org/10.33263/LIANBS91.779783.